

## Dosimetric Study of an Indigenous and Heterogeneous Pelvic Phantom for Radiotherapy Quality Assurance

Sudha Singh<sup>1</sup>, Payal Raina<sup>1\*</sup>, Om Prakash Gurjar<sup>2</sup>

1. Department of Physics, Ranchi University, Ranchi – 834008, Jharkhand
2. Government Cancer Hospital, Mahatma Gandhi Memorial Medical College, Indore - 452001, Madhya Pradesh, India

| ARTICLE INFO   | ABSTRACT   |
|--|--|
| <b>Article type:</b><br>Original Article   | <b>Introduction:</b> In vitro dosimetric verification prior to patient treatment plays a key role in accurate and precision radiotherapy treatment delivery. Since the human body is a heterogeneous medium, the aim of this study was to design a heterogeneous pelvic phantom for radiotherapy quality assurance.  |
| <b>Article history:</b><br>Received: Mar13, 2019<br>Accepted: Jun 08, 2019                   | <b>Material and Methods:</b> A pelvic phantom was designed using wax, pelvic bone, borax powder, and water mimicking different biological tissues. Hounsfield units and relative electron densities were measured. Various intensity-modulated radiotherapy (IMRT) plans were imported to the pelvic phantom for verification and implemented on the Delta 4 phantom. The quantitative evaluation was performed in terms of dose deviation, distance to agreement, and gamma index passing rate.   |
| <b>Keywords:</b><br>Algorithm<br>Phantom<br>CT Number<br>Intensity Modulated<br>Radiotherapy | <b>Results:</b> According to the results of the CT images of an actual patient, relative electron densities for bone, fat, air cavity, bladder, and rectum were 1.335, 0.955, 0.158, 1.039, and 1.054, respectively. Moreover, the CT images of a heterogeneous pelvic phantom showed the relative electron densities for bone, fat (wax), air cavity, bladder (water), and rectum (borax powder) as 1.632, 0.896, 0.159, 1.037, and 1.051, respectively. The mean percentage variation between planned and measured doses was found to be 2.13% within the tolerance limit (<math>\pm 3\%</math>). In all test cases, the gamma index passing rate was greater than 90%.<br><b>Conclusion:</b> The findings showed the suitability of the materials used in the design of the heterogeneous phantom. Therefore, it can be concluded that the designed phantom can be used for regular radiotherapy quality assurance. |

► Please cite this article as:

Singh S, Raina P, Gurjar OP. Dosimetric Study of an Indigenous and Heterogeneous Pelvic Phantom for Radiotherapy Quality Assurance. Iran J Med Phys 2020; 17: 120-125. 10.22038/ijmp.2019.39332.1520.

### Introduction

The success of therapeutic external beam radiation therapy depends on the spatial dose distribution in the patient [1, 2]. Since the energy deposition is three dimensional in nature, the particles not only interact with the tumor site but also deposit some of their energy into the adjacent area [3]. Consequently, neighboring normal tissues also receive some amount of radiation dose in this process. Therefore, normal tissue dose tolerance becomes a limiting factor for successful treatment.

The dose distribution given by intensity-modulated radiotherapy (IMRT) is highly conformal, compared to conventional radiotherapies; however, due to the presence of the large numbers of fields and irregular shape and size of the treatment segments, the accuracy of IMRT delivery needs to be verified via dose measurement. Different dosimetry techniques are available to compare the planned dose with a delivered dose [4,5] using an ionization chamber and commercially available phantom, such as slab phantom that measures the point dose at a particular desired reference depth. For reference dosimetry, radiographic or radiochromic film is placed at a

particular depth in a slab phantom, and the planned dose is delivered on it. The film quality assurance (QA) dosimetry system, for instance, Omni Pro IMRT correlates the resultant density of film with the planned dose at each point.

Luminescence dosimetry is also performed using optically stimulated luminescence (OSL) system and thermoluminescent dosimeters (TLD). It can be also used for in vivo dosimetry in which OSL or TLD are placed on the patient body at reference points for measurement. The electronic portal imaging device is also utilized for reference dosimetry [6,7]. In addition, many detector based phantoms are available for reference dosimetry, such as Accua Check and Delta 4 phantom. The majority of the commercially available phantoms are of homogeneous density, whereas the actual human body is a complex medium of different density patterns [8]. Additionally, the very few heterogeneous phantoms which are available commercially (i.e., anthropomorphic phantoms) are very costly which are not procured by most of the radiotherapy centers, especially in developing countries.

\*Corresponding Author: Email: payalraina2008@gmail.com

Based on the recommendations of International Atomic Energy Agency published in technical reports series (No: 277 and 398) [9,10], there are several techniques to attain accuracy in dosimetry. It is known that human body is composed of fat, tissue, bones, and, air cavities having different electron density that influences the interaction of photon and electron energy deposition affecting the dose delivery to a target volume. As a result, it is essential to stabilize the quality dosimetric practice followed by pre-treatment verification. Therefore, this study was conducted to develop an indigenous and heterogeneous pelvic phantom similar to patient anatomy and perform a pre-treatment verification in a realistic clinical scenario to obtain reproducible dosimetry.

## Materials and Methods

### Designed phantom

In this study, a heterogeneous pelvic phantom was designed (Figure 1) which was made of wax, a male pelvic bone (Figure 2), water, and borax powder. To construct the phantom, a male pelvic bone with a density equivalent to that of a human pelvic bone was placed in a cylindrical-shaped container. After placing it around a plastic ball, it was filled with water and placed for bladder. Borax powder with glue and water were placed below the bladder for rectum. Subsequently, molten wax was poured into it and allowed to solidify. After complete solidification of the wax, the outer container was cut and removed. A cavity was prepared at approximately geometrical centre of the phantom volume, and a 0.6 cm<sup>3</sup> ion chamber was kept in the same position until the end of the experiment (Figure 3).

The prostate was not considered because a cavity was made at the phantom centre, and the 0.6 cm<sup>3</sup> ion chamber (PTW, Freiburg, Germany) was placed for the verification of IMRT for patients with prostate; moreover, the Hounsfield Unit (HU) of rectum and prostate was almost equal. The three fiducially lead markers were put on the two bilateral points, and one anterior point was placed on the surface of the phantom in the same cross-sectional plane to make three reference points.

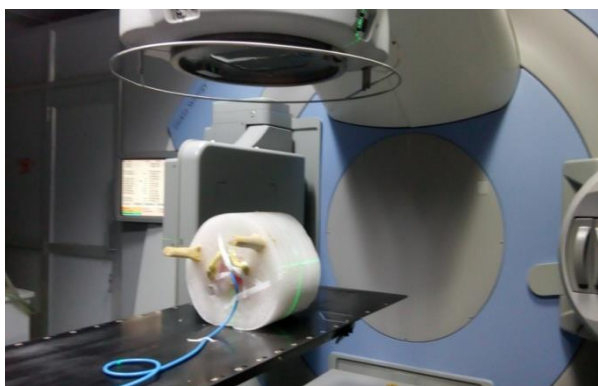


Figure1. A designed pelvic phantom



Figure 2. A male pelvis and femur bone used in a developed phantom

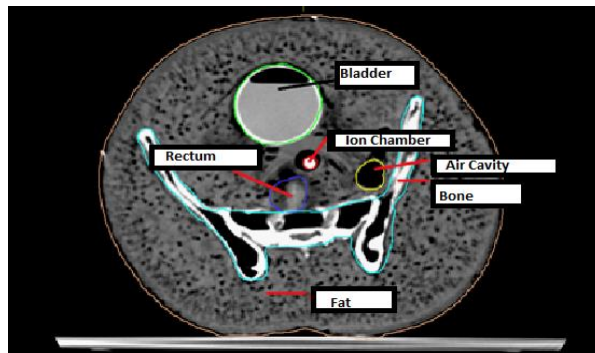


Figure3. CT slice of a developed phantom with different parts

Brivo CT 325 2-slice (GE Healthcare, WI, USA) has been utilized for computed tomography (CT) of the phantom and the CT images were taken at a slice thickness of 3 mm for planning purposes. Subsequently, the images were imported to a treatment planning system (TPS). The width and height were measured using the length measuring tool available in the TPS. The mean width and height were measured as 29 and 25 cm in the CT images of a heterogeneous pelvic phantom, respectively. These geometries of the phantom show that it can accommodate delivered beam field sizes and shapes. It allows the establishment of 3D locations. It is easy to transport, set up, align, and take down in an accurate and efficient manner.

### Hounsfield Unit and Relative Electron Density

The substitute material's CT numbers at 120 kVp and 130 mAs were measured at the CT scanner console. Elliptical region of interest with an area of 80.3 mm<sup>2</sup> was taken for the measurement. Moreover, TPS lookup table was used with the volume cursor in Monaco planning system (version 3.1, Elekta Ltd, Crawley, UK) to convert the HU to a relative electron density. HU and relative electron density were evaluated by using CT scanner console with considering the density variation in different CT slices. For actual patient, HU and relative electron density variation were calculated from CT image of one patient.

### Intensity-modulated radiotherapy planning

Various IMRT plans for prostate patients were generated on a Monaco planning system. Plans were created with 5, 7, 9, and 12 coplanar 6MV photon

beams. Couch and collimator angles were kept at  $0^\circ$  for all plans. Calculation parameters, such as grid spacing, fluence smoothing, and statistical uncertainty were 0.3 cm, medium, and 1% per plan, respectively. Furthermore, the Monte Carlo algorithm was used for the plan optimization, and all the plans were generated in a step and shoot mode.

### Gamma analysis

The difference between measured and planned dose distribution is evaluated using quantitative evaluation methods. The QA procedures of TPS narrated by Van Dyk et al. [11] subdivides the dose distribution comparisons into high and low dose gradients regions, each with a different acceptance standard. In regions of low gradient, planned and measured doses are compared directly with an acceptable tolerance placed on the difference between the measured and calculated doses. On the other hand, in high dose gradient regions, a small spatial error either in measurement or calculation results in a large dose difference between measurement and calculation. Therefore, in the region of high dose gradient, the concept of a distance-to-agreement (DTA) distribution is used to determine the acceptability of the dose calculation [12]. The DTA is the distance between a measured data point and the nearest point in the calculated dose distribution exhibiting the same dose. The dose difference (DD) and DTA evaluations complement each other when used as determinants of dose distribution calculation quality. Gamma criteria of 3% DD and 3 mm DTA were used in this study to evaluate IMRT treatment plans.

### Delta4 phantom

All test cases investigated in this study were planned and delivered on Delta4 Phantom (Scandidos, Uppsala, Sweden). Delta4 is a cylindrical and polymethylmethacrylate phantom consisting of two orthogonal detector planes in a crossed array. It consists of 1069 p-type silicon diodes that can measure point doses and can be used for QA. The detector planes spatial resolution is 5 mm at the central area of  $6 \times 6$  cm and 10 mm at the outer area in each plane. The cylindrical phantom has a diameter and length of 22 and 40 cm, respectively [13]. Dose difference, DTA and gamma index were evaluated by using Delta 4 phantom.

### Pre-treatment verification

After the complete optimization of the IMRT, the plans were exported to a pelvic phantom and Delta4 phantom for a pre-treatment verification. After position verification, all IMRT plans were delivered by a linear accelerator. In a pelvic phantom, the dose for each plan was measured using PTW UNIDOS E electrometer connected with 0.6 cm<sup>3</sup> ion chamber according to International Atomic Energy Agency (IAEA) published, Technical Reports Series-398 (TRS 398) protocol. These measured doses were compared with doses planned on TPS. For Delta4 phantom, TPS calculated dose fluence was compared with measured dose fluence using gamma evaluation method with critically acceptable criteria of 3 mm DTA and 3% DD. Before the evaluation of an IMRT plan, two more measurements were done by delivering 100 cGy with a  $10 \times 10$  cm field at gantry angles of  $0^\circ$  and  $90^\circ$  in order to check the phantom for positional corrections and linac output constancy.

## Results

The HU and relative electron density of bone, fat, air cavity, bladder, and rectum in CT images of a heterogeneous phantom and an actual patient were measured and given in Table 1. All the measurements were calculated by using CT scanner console in terms of mean and standard deviation due to density variation in different CT slices. For actual patient, CT image of one patient was taken. According to the results obtained from the CT images of a heterogeneous pelvic phantom, relative electron densities for bone, fat (wax), air cavity, bladder (water), and rectum (borax powder) were 1.632, 0.896, 0.159, 1.037, and 1.051, respectively. On the other hand, relative electron densities for bone, fat, air cavity, bladder, and rectum were 1.335, 0.955, 0.158, 1.039, and 1.054, respectively, in an actual patient CT image.

Table 2 tabulates the planning parameters, including a number of fields, segments and monitor units, and the percentage variation between planned doses and measured doses for each test case using pelvic phantom. Moreover, the gamma analysis results using Delta 4 of each test case, including DD, DTA, and gamma index passing rates are presented in table 3.

Table 1. Comparison of Hounsfield Units and relative electron densities of organs

| S.No. | Pelvic Organs | Material         | In CT images of a heterogeneous phantom |                           | In CT images of an actual patient |                           |
|-------|---------------|------------------|---|---------------------------|-----------------------------------|---------------------------|
|       |               |                  | HU $\pm$ SD                             | Relative electron density | HU $\pm$ SD                       | Relative electron density |
| 1     | Bone          | Male Pelvic Bone | 1037 $\pm$ 179                          | 1.632                     | 556 $\pm$ 187                     | 1.335                     |
| 2     | Fat           | Wax              | -162 $\pm$ 45                           | 0.896                     | -109 $\pm$ 108                    | 0.955                     |
| 3     | Air cavity    | Air              | -846 $\pm$ 143                          | 0.159                     | -847 $\pm$ 79                     | 0.158                     |
| 4     | Bladder       | Water            | -5 $\pm$ 5                              | 1.037                     | -3 $\pm$ 8                        | 1.039                     |
| 5     | Rectum        | Borax Powder     | 19 $\pm$ 53                             | 1.051                     | 20 $\pm$ 26                       | 1.054                     |

CT: Computed Tomography; HU: Hounsfield Units; SD: Standard Deviation.

Table 2. Percentage variation between planned dose on the treatment planning system and measured dose on linear accelerator using a heterogeneous pelvic phantom

| Plan No.  | Algorithm   | Energy | No. of fields | Measured Dose | Planned Dose | % Variation |
|-----------|-------------|--------|---------------|---------------|--------------|-------------|
| P1        | Monte Carlo | 6 MV   | 5             | 190.34        | 185.8        | 2.44 (+)    |
| P2        | Monte Carlo | 6 MV   | 7             | 202.15        | 207.5        | 2.58(-)     |
| P3        | Monte Carlo | 6 MV   | 9             | 172.46        | 176.1        | 2.07(-)     |
| P4        | Monte Carlo | 6 MV   | 12            | 194.57        | 191.84       | 1.42(+)     |
| Mean 2.13 |             |        |               |               |              |             |
| SD 0.52   |             |        |               |               |              |             |

MV: Mega Voltage; SD: Standard Deviation

Table 3. Result of dose difference, distance to agreement, and gamma index using Delta 4 phantom

| Plan No. | Field Number | Segment Number | Monitor Unit | Dose Difference | DTA   | Gamma Index |
|----------|--------------|----------------|--------------|-----------------|-------|-------------|
| P1       | 5            | 14             | 734.20       | 80.5%           | 95.2% | 97.8%       |
| P2       | 7            | 19             | 820.31       | 80.1%           | 95.1% | 97.3%       |
| P3       | 9            | 15             | 775.48       | 81.4%           | 94.3% | 97.5%       |
| P4       | 12           | 14             | 724.53       | 80.8%           | 95.3% | 98.8%       |

DTA: Distance to agreement

**Test case P1: IMRT plan with 5 coplanar beams**

The percentage variation between planned doses and measured doses was noted as 2.44% in a designed pelvic phantom. The same plan was verified using Delta 4 phantom. The gamma passing rate for test P1 was 97.8%, whereas the pass percentages of DD and DTA were 80.5% and 95.2%, respectively.

**Test case P2: IMRT plan with 7 coplanar beams**

The percentage variation between planned doses and measured doses was noted as 2.58% in a designed pelvic phantom. The same plan was verified using Delta 4 phantom. The gamma passing rate for test P2 was 97.3%, whereas the pass percentages of DD and DTA were 80.1% and 94.3%, respectively. Dose distribution at the axial projection on a heterogeneous phantom, Delta 4phantom, and an actual patient CT image were shown in figures 4, 5, and 6, respectively. The gamma index results using Delta 4 phantom are provided in figure 7.

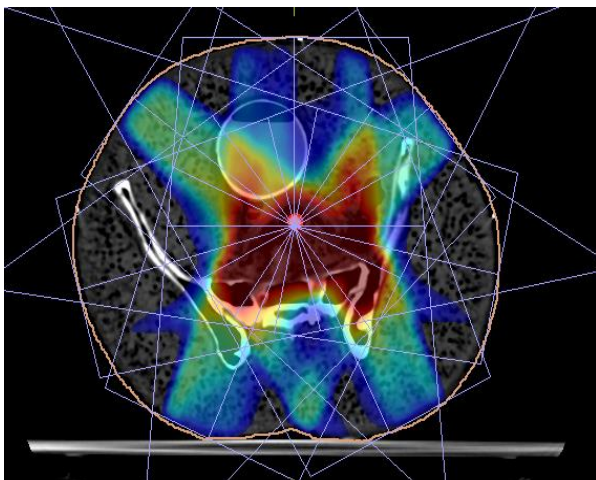


Figure 4. Dose distribution in a heterogeneous phantom CT slice for test case P2

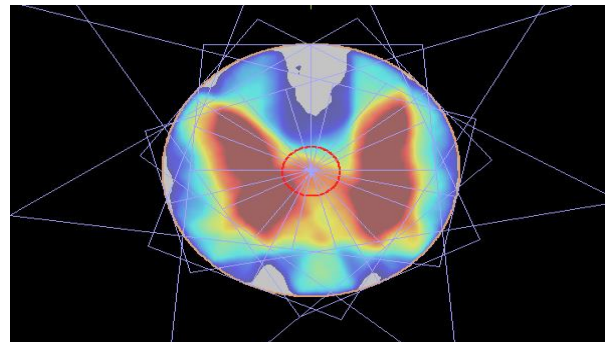


Figure 5. Dose distribution in a Delta4 phantom CT slice for test case P2

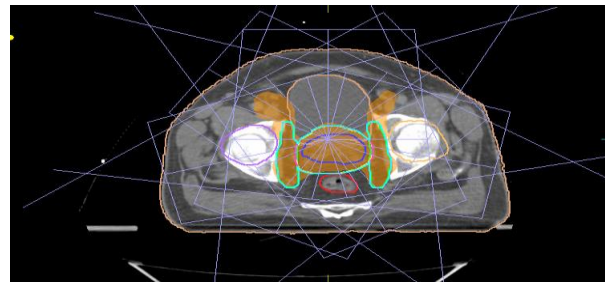


Figure 6. Dose distribution in a patient CT for test case P2

**Test case P3: IMRT plan with 9 coplanar beams**

Similarly, with 9 coplanar beams, the percentage variation between planned doses and measured doses was noted as 2.07%. The DD, DTA, and gamma index were 81.4%, 94.3%, and 97.5%, respectively.

**Test case P4: IMRT plan with 12 coplanar beams**

For the IMRT with 12 coplanar beams, the percentage variation between planned doses and measured doses was noted as 1.42%. The DD, DTA, and gamma index were 80.8%, 95.3%, and 98.8%, respectively.

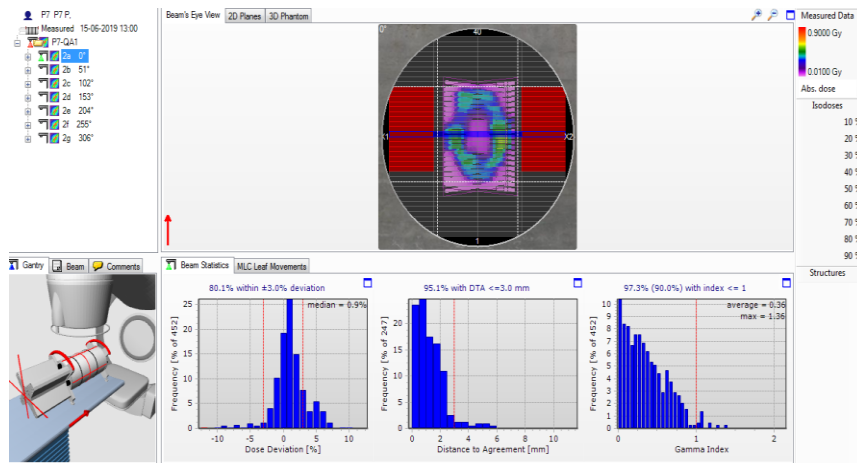


Figure 7. Dose distribution, dose deviation, distance to agreement, and gamma index of test case P2

## Discussion

This study attempted to develop an indigenous and inhomogeneous three-dimensional pelvic phantom for dosimetric verification. The purpose of this study was to compare the CT number and electron density of the developed phantom with an actual patient CT image. Moreover, this study investigated the effects of tissue heterogeneities in dose calculation. The materials used for the construction of the phantom were easily available with affordable price and the result of this study revealed that the fabricated phantom was similar to an actual patient.

OP Gurjar et al. [14] evaluated the materials dosimetrically to prepare a heterogeneous body phantom; however, in the present study, the phantom was prepared using different suitable materials and tested in a similar way. An anthropomorphic pelvic phantom using acrylic plates and suitable material for radiotherapy QA was designed by P Shokraine et al. [15] similar to the technique used in this study. Moreover, F Zhang et al. designed and fabricated a personalized anthropomorphic phantom using 3D printing [16]. They used tissue-equivalent materials for designing the phantom.

Furthermore, the TPS algorithms were validated with the ion chamber in the phantom. Similar to our study, the CT number (HU) was also compared with that of an actual patient CT. The relative electron density of bladder, rectum, fat, bone, and cavities was also estimated by D Shrotriya et al. [17] which were reported to be 1.305, 1.0247, 0.9132, 1.5786, and 0.7791, respectively. These results are also in line with observed values of 1.037, 1.051, 0.896, 1.632, and 0.159, respectively, with a small deviation in this study.

In the same line, MO Akpochafor *et al.* [18] has also developed a pelvic phantom for the verification of a TPS using convolution, fast superposition, and superposition algorithms. The mean percentage deviation recorded in their study was obtained at  $\pm 4\%$ ; however, the mean percentage deviation in this study was estimated at  $\pm 3\%$  which was within the tolerance limit ( $< \pm 3\%$ ) prescribed in the International Commission on Radiation Units and

Measurements-83. Additionally, Gamma evaluation results were also within the critically acceptable criteria of 3 mm DTA and 3% DD (Table 3).

As can be seen in Table 1, it can be stated that the values of HU and relative electron densities for different materials in the heterogeneous phantom are equivalent to that of the organs in an actual human pelvis. Therefore, the selection of the materials for phantom preparation was rational. Dosimetric analysis and the cost-effectiveness of the indigenous phantom permit us to utilize it for the QA in radiotherapy.

## Conclusion

In the present study, an indigenous and heterogeneous male pelvic phantom was made and the results showed the similarity between its density pattern and that of the actual patient pelvic region. Materials used for the construction of phantom were locally available, cost-effective, and strong enough to maintain structural integrity. The percentage variations between planned and measured doses were within the tolerance limit in all the test cases ( $< \pm 3\%$ ), and gamma index value was also within the tolerance limit ( $> 90\%$ ). This shows that the materials used in the design of a heterogeneous phantom were suitable and that the phantom can be used successfully for verification practices. Furthermore, the cost of designing the phantom is minimal, and it is easier to use. Additionally, this phantom will improve radiotherapy QA practices.

## Acknowledgment

The corresponding author would like to acknowledge the co-operation of Dr. Anup Kumar, the Head of the Department of Radiation Oncology, Ranchi, India, for providing the facilities. The authors are also thankful to Mr. S. K. Sahoo, Radiotherapy Technologist of the Department for his support in taking measurements.

## References

1. Bentzen SM, Overgaard J. Patient-to-Patient Variability in the Expression of Radiation-Induced Normal Tissue Injury. *Semin Radiat Oncol*. 1994;4(2):68-80.
2. Brahme A. Dosimetric precision requirements in radiation therapy. *Acta Radiol Oncol*. 1984;23(5):379-91.
3. Brahme A. Design principles and clinical possibilities with a new generation of radiation therapy equipment. A review. *Acta Oncol*. 1987;26(6):403-12.
4. Bouchard H, Seuntjens J. Ionization chamber-based reference dosimetry of intensity modulated radiation beams. *Med Phys*. 2004;31:2454-65.
5. Fraser D, Parker W, Seuntjens J. Characterization of cylindrical ionization chamber for patient specific IMRT QA. *J Appl Clin Med Phys*. 2009;10(4):241-51.
6. Nijsten SM, Mijneer BJ, Dekkar AL, Lambin P, Minken AW. Routine individualised patient dosimetry using electronic portal imaging devices. *Radiother Oncol*. 2007;83:65-75.
7. Huang YC, Yeh CY, Yeh JH, Lo CJ, Tsai PF, Hung CH, et al. Clinical practice and evaluation of electronic portal imaging device for VMAT quality assurance. *Med Dosim*. 2013;38:35-41.
8. Gurjar OP, Mishra SP, Bhandari V, Pathak P, Patel P, Shrivastav G. Radiation dose verification using real tissue phantom in modern radiotherapy techniques. *J Med Phys*. 2014;39(1):44-9.
9. IAEA. Absorbed dose determination in photon and electron beams, An International Code of Practice. Series No. 277. Vienna; 1997.
10. IAEA. An International Code of Practice for Dosimetry based on absorbed dose to water: Series No. 398, absorbed dose determination in external beam radiotherapy. Vienna; 2000.
11. Van Dyk J, Barnett RB, Cygler JE, Shragge PC. Commissioning and quality assurance of treatment planning computers. *Int J Radiat Oncol Biol Phys*. 1993; 26:261-73.
12. Harms WBSr, Low DA, Wong WJ, Purdy JA. A software tool for the quantitative evaluation of 3D dose calculation algorithms. *Med Phys*. 1998;25(10):1830-6.
13. Avgousti R, Armpilia C, Floros I, Antypas C. Evaluation of intensity modulated radiation therapy delivery system using a volumetric phantom on the basis of the task group 119 report of American association of physicists in medicine. *J Med Phys*. 2017;42:33-41.
14. Gurjar OP, Paliwal RK, Mishra SP. A dosimetric study on slab-pine-wood-slab phantom for developing the heterogeneous chest phantom mimicking actual human chest. *J Med Phys*. 2017;42(2):80-5.
15. Schaly B, Varchena V, Au P, Pang G. Evaluation of an anthropomorphic male pelvic phantom for image-guided radiotherapy. *Reports in Medical Imaging*. 2009; 2:69-78.
16. Zhang F, Zhang H, Zhao H, He Z, Shi L, He Y, et al. Design and fabrication of a personalized anthropomorphic phantom using 3D printing and tissue equivalent materials. *Quant Imaging Med Surg*. 2019;9(1):94-100.
17. Shrotriya D, Yadav RS, Srivastava RNL, Verma TR. Design and Development of an Indigenous In-house Tissue-equivalent Female Pelvic Phantom for Radiological Dosimetric Applications. *Iran J Med Phys*. 2018; 15:200-5.
18. Akpochafor MO, Madu CB, Habeebu MY, Omojola AD, Adeneye SO, Aweda MA. Development of pelvis phantom for verification of treatment planning system using convolution, fast superposition, and superposition algorithms. *J Clin Sci*. 2017; 14:74-80.